HHS Public Access

Author manuscript

NMR Biomed. Author manuscript; available in PMC 2016 June 01.

Published in final edited form as:

NMR Biomed. 2015 June ; 28(6): 633–641. doi:10.1002/nbm.3291.

Quantification of in vivo ^{31}P NMR Brain Spectra using LCModel

Dinesh Kumar Deelchand[1], **Tra My Nguyen**[2], **Xiao-Hong Zhu**[1], **Fanny Mochel**[2,3,4], and **Pierre-Gilles Henry**[1]

[1]Center for Magnetic Resonance Research, University of Minnesota, Minneapolis, MN, United States

[2]INSERM UMR S975, Brain and Spine Institute, Hospital La Salpêtrière, Paris, France

[3]University Pierre and Marie Curie, Paris, France

[4]AP-HP, Department of Genetic, Hospital La Salpêtrière, Paris, France

Abstract

Quantification of ^{31}P NMR spectra is commonly performed using line-fitting techniques with prior knowledge. Currently available time- and frequency- domain analysis software includes AMARES (in jMRUI) and CFIT respectively. Another popular frequency domain approach is LCModel, which has been successfully used to fit both ^{1}H and ^{13}C in vivo NMR spectra. To the best of our knowledge LCModel has not been used to fit ^{31}P spectra. This study demonstrates the feasibility of using LCModel to quantify in vivo ^{31}P MR spectra, provided that adequate prior knowledge and LCModel CONTROL parameters are used. Both single-voxel and MRSI data are presented and similar results are obtained with LCModel and with AMARES. This provides a new method for automated, operator-independent analysis of ^{31}P NMR spectra.

Graphical abstract

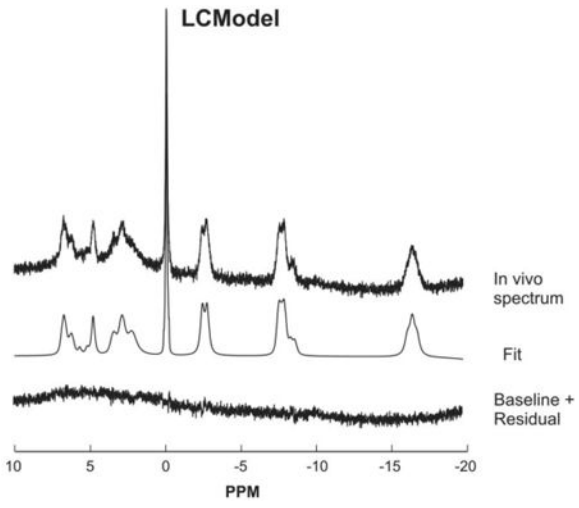

Proofs and reprint requests to: Dinesh K. Deelchand, Ph.D. Center for Magnetic Resonance Research, University of Minnesota, 2021 6th St SE, Minneapolis, MN 55455, USA, Phone: (1) 612-626-2001, Fax: (1) 612-626-2004, deelc001@umn.edu.

LCModel can successfully fit in vivo ^{31}P spectra (both single-voxel and MRSI data) when the appropriate basis set and the differences in the apparent linewidths for each metabolite are taken into account. Example of an LCModel fitted ^{31}P spectrum (acquired from the human brain at 3 Tesla) is shown here.

Keywords

^{31}P; animal; AMARES; brain; human; jMRUI; LCModel; MRSI

Introduction

In vivo NMR spectroscopy (MRS) allows noninvasive measurements of the concentration of brain metabolites in humans and animals. In particular, phosphorus MRS (^{31}P MRS) is commonly used to detect key energy metabolites such as adenosine triphosphate (ATP), phosphocreatine (PCr) and inorganic phosphate (Pi). It also allows determination of intracellular pH (based on the difference between the chemical shifts of PCr and Pi (1)) and measurement of metabolic reaction fluxes using magnetization transfer technique (2).

To extract all of the relevant information provided by ^{31}P MRS, the NMR spectra need to be accurately quantified. For ^{31}P spectral analysis, several techniques have been reported which can be performed in either the time or frequency domain.

A popular time-domain line-fitting method is AMARES (Advanced Method for Accurate, Robust and Efficient Spectral fitting) (3), in which prior knowledge (e.g. chemical shift, linewidth, amplitude and phase information) for each resonance is included in order to obtain a reliable fit (4). AMARES is part of the jMRUI package, which is free for academic use. Another available method uses a Marquardt-Levenberg algorithm after obtaining prior knowledge with a Hankel singular value decomposition (HSVD) algorithm (5,6). In both of these techniques, the prior knowledge was derived from high signal-to-noise ^{31}P NMR spectra generally obtained by summing data from several subjects. This prior knowledge was then used to quantify lower signal-to-noise spectra.

A variant of HSVD (known as IRIS-HSVD (7)) was recently shown to be useful when analyzing ^{31}P spectra with distorted baseline. This algorithm iteratively fits all resonances along with the baseline until the residual is minimized. In this case, the prior knowledge was also estimated using HSVD. IRIS-HSVD was reported to have significantly smaller mean and standard deviation for resolving the peaks of interest around the true chemical shift values compared to AMARES (7).

Analysis of ^{31}P data in the frequency domain has been reported using CFIT (8). This technique fits the circular trajectories of the peaks (when projected onto the complex plane) with active circle models where prior knowledge is incorporated as constraint energy terms. A comparison between CFIT and AMARES on in vivo ^{31}P spectra reported a higher fitting failure rate and lower fitting accuracy with AMARES than with CFIT due to presence of baseline artifacts (8). TDFDFIT is another frequency domain technique which uses time-domain models (9) derived from high signal-to-noise ^{31}P NMR spectra (10).

Another frequency domain approach is LCModel (11), a commercial software in which the in vivo spectrum is approximated as a linear combination of model spectra of different metabolites present in the measured spectrum. These spectra can be acquired in vitro using the same pulse sequence as used for the in vivo measurement, or they can be simulated based on known chemical shifts and *J*-coupling values. Over the last decade, LCModel has been widely used to fit in vivo ^{1}H NMR spectra in both human and rodent brains (12,13). It was further extended to quantify in vivo ^{13}C spectra (14,15), but to the best of our knowledge this technique has not been used to fit ^{31}P NMR spectra. Therefore, the aim of this study was to evaluate the suitability of LCModel to quantify in vivo ^{31}P NMR spectra. The method is demonstrated by fitting ^{31}P MR spectra from human brain at 3 Tesla, and validated by comparing quantification results with those obtained with AMARES. Quantification of magnetic resonance spectroscopic imaging (MRSI) data from human brain at 7 Tesla and localized single-voxel data from mouse brain at 9.4 Tesla are also shown.

Methods

In vivo ^{31}P MR Spectroscopy at 3 Tesla

Healthy volunteers (N = 10) were studied on a 3 Tesla whole-body Siemens Trio (Siemens Medical Solutions, Erlangen, Germany). Informed consent was obtained from all participants prior to the study. The standard Siemens body ^{1}H RF coil was used for ^{1}H imaging and B_0 shimming, and a small transceiver ^{31}P surface coil (6 cm diameter, Rapid biomedical GmbH, Germany) was used for ^{31}P MRS. The subjects lay in a supine position with their head placed above the ^{31}P RF coil. A small sphere filled with water was placed at the center of the ^{31}P RF coil to verify the precise positioning of the ^{31}P coil on ^{1}H images.

T_1-weighted ^{1}H images were first acquired from the brain followed by adjustment of the position of the ^{31}P coil such that the water sphere was aligned with the center of the visual cortex. Localized automatic B_0 shimming was then performed on a 3×3×3 cm^3 voxel placed in the primary visual cortex area resulting in water line width between 14 Hz and 18 Hz.

In vivo unlocalized ^{31}P NMR spectra (without ^{1}H decoupling) were acquired from the occipital cortex using a pulse-acquire sequence (square excitation RF pulse) and a repetition time (T_R) of 2 s. For each subject, the excitation flip angle in the region-of-interest was adjusted to approximately 60° (close the Ernst angle for PCr and Pi with T_R = 2 s). ^{31}P signals were then acquired (600 scans) using a spectral width of 2 kHz and 2048 complex data points. To achieve steady-state magnetization, four dummy scans were acquired at the beginning.

Spectral Processing

All ^{31}P spectra were processed using Matlab (The MathWorks Inc., Natick, MA, USA). Spectra from each subject were manually phased (zero- and first-order correction). Single-shot frequency correction was performed automatically using a cross-correlation algorithm. The summed spectrum was referenced by placing the PCr peak at 0 ppm.

LCModel Analysis

All spectra were analyzed using LCModel version 6.3-0G (Stephen Provencher Inc., Oakville, ON, Canada) (11). Basis spectra were simulated using home-written programs in Matlab using published (5,6,14,16,17) and measured ^{31}P chemical shifts and ^{31}P-^{31}P *J*-coupling (J_{PP}) and long-range ^{31}P–^{1}H *J*-coupling (J_{PH}) constants (Table 1). For the basis set generation, LCModel requires that each basis spectrum has a singlet peak for referencing and by default LCModel uses the 0.0 ppm chemical shift. However, in ^{31}P NMR, this chemical shift (i.e. 0.0 ppm) is generally assigned to the PCr singlet peak. Therefore, when generating LCModel basis spectra for ^{31}P in this study, the reference peak was set at -25.0 ppm (i.e. PPMPK = - 25, the chemical shift (in ppm) of the reference peak used in LCModel when generating the basis set).

The model basis set consisted of 13 basis spectra: PCr, α-ATP, β-ATP, γ-ATP, Pi, nicotinamide adenine dinucleotide (reduced form, NADH and oxidized form, NAD^+), phosphorylethanolamine (PE), phosphorylcholine (PC), glycerol-3-phosphorylethanolamine (GPE), glycerol-3-phosphorylcholine (GPC), membrane phospholipids (MP) and 2,3-diphosphoglycerate (DPG). Phase evolution due to J_{PP} coupling was neglected as the data was acquired with a pulse-acquire sequence. With a POCE type sequence, dephasing due to J_{PP} coupling could be incorporated as prior knowledge into the basis set as demonstrated earlier for ^{13}C POCE spectra (14). Two different basis sets were generated: 1) a “fixed linewidth” basis set in which all metabolite basis spectra were simulated with a fixed linewidth of 2 Hz and 2) an “adjusted linewidth” basis set in which each metabolite spectrum was simulated with a linewidth equal to the average measured in vivo linewidth (Table 2) minus 3 Hz for all metabolites. The average in vivo linewidth was estimated by fitting multiple in vivo spectra using the “fixed linewidth” basis set. The linewidth of each metabolite in the in vivo spectrum was then available in the LCModel.PRINT output file.

Three methods were utilized during the fitting procedure: LCModel approach #1 uses the “fixed linewidth” basis set together with default LCModel broadening parameters DEEXT2 = 2 Hz and DESDT2 = 0.4 Hz. These parameters specify the expected mean and standard deviation of line broadening from the basis set spectra to the in vivo spectrum. LCModel approach #2 uses the same “fixed linewidth” basis set, but with DEEXT2 = 10 Hz and DESDT2 = 10 Hz, giving more flexibility to LCModel for line broadening. LCModel approach #3 uses the “adjusted linewidth” basis set with DEEXT2 = 2 Hz and DESDT2 = 0.4 Hz.

For the preliminary LCModel analysis, the following three resonances were chosen: PCr, Pi and α-ATP. As previously reported for ^{13}C fitting using LCModel (14), the following input parameters were used: DKNTMN = 2*99; XSTEP = 5; RFWHM = 3; FWHMBA = 0.049; NREFPK(2) = 1; PPMREF(1,2) = 0; DESDSH = 0.01. The default values which define the spline baseline function were also adjusted in order to take account of the larger ppm range of ^{31}P compared to ^{1}H: ALPBMN = 7.8e-10, ALPBMX = 3.9e-7, ALPBPN = 9.8e-10, ALPBST = 1.2e-9 (11). In addition, the standard deviations on the zero- and first- order phases were set to SDDEGZ = 3 and SDDEGP = 0.4 respectively in order to allow small phase flexibility. No baseline correction, zero-filling or apodization functions were applied

to the in vivo data prior to the analysis. LCModel fitting was performed over the spectral range from -19.5 to 10 ppm. At 3 Tesla, NAD^+ and NADH cannot be fitted separately and only their sum (tNAD = NAD^+ + NADH) is reported.

AMARES Analysis

^{31}P spectra were also analyzed using the AMARES algorithm available in jMRUI (18) with prior knowledge. All peaks were fitted using a Lorentzian line shape. α-ATP, γ-ATP, DPG and NAD^+ were each modeled as doublets with identical amplitude while β-ATP consisted of three singlets with an amplitude ratio of 1:2:1. The rest of the metabolites were considered as singlets. The frequencies of all metabolites were constrained to ±0.05 ppm based on their chemical shift reported in Table 1, except for the two resonances of the NAD^+ doublet which had a fixed frequency shift of -19 Hz and 1.0 Hz respectively relative to NADH. Furthermore, the linewidth of all metabolites were constrained to be between 5 and 15 Hz except for MP which was between 25 and 40 Hz. The zero-order phase was constrained between -20° to 20° while the first-order phase was constrained between -0.5 ms to 0.5 ms in the time domain. To reduce the effect of the baseline, frequency-selective weighting (quarter-sine wave) was applied to the first 20 points in the time domain. In addition, the first 2 points were truncated during the fit.

Statistical Analysis

Differences in metabolite concentrations between LCModel and AMARES were analyzed using a two-tailed equal variance Student's *t*-test. Differences were considered statistically significant if $P < 0.05$, with Bonferroni correction for multiple comparisons. In addition, the Spearman's rank correlation coefficient was used to estimate the correlation of metabolite concentrations between the two methods.

^{31}P MRSI

One healthy volunteer was scanned in a 7 Tesla/90 cm bore scanner (Siemens Medical Solutions, Erlangen, Germany) after providing informed consent. A home-built RF coil used consisted of a large ^1H coil for anatomic imaging and B_0 shimming and a small transceiver ^{31}P surface loop (~5cm diameter) was used for ^{31}P MRS. The subject lay in a supine position with the head (visual cortex) placed above the ^{31}P RF coil. After acquiring T_1 images and performing localized B_0 shimming as described above, 3D Fourier series window ^{31}P MRSI spectra were acquired using the following parameters: FOV = 12×12×9 cm^3, matrix size = 7×7×5, T_R = 1.2 s, 300 μs hard pulse (average flip angle ~70° in the visual cortex), total scan = 2240 and nominal voxel size of 5.3 cm^3.

MRSI data were processed in Matlab; automatic zero- and first- order phase corrections were performed in each voxel only if the peak SNR of PCr was > 5 in that voxel. Then ^{31}P spectra from each voxel were analyzed with LCModel as described above.

^{31}P Mouse MRS

Localized ^{31}P spectra were acquired using a 3D ISIS localization sequence at 9.4 T in 4 wild-type mouse brain (volume-of-interest (VOI) of 5×3×5 mm^3 positioned in the dorsal

region) as reported previously (19). After frequency and phase corrections, the summed spectrum from the 4 animals was analyzed using LCModel.

Measurement of J_{PH} Coupling Constants

^{31}P - ^{1}H *J*-coupling values in PE, GPE and GPC were measured in vitro. Brain extract from one rat was prepared as previously described in Henry (14). Briefly, after suspending in 10% D2O and pH adjusted (range 7.10–7.20), ^{31}P NMR spectra were recorded from the extract at 37°C on a 14.1 Tesla INOVA spectrometer (Agilent Technologies, CA) using a pulse-acquire sequence (repetition time of 3 s and 24,960 averages). Based on the measured T_1 of PCr of about 3.5 s, a 65° flip angle was used for optimal SNR. Line broadening of 0.5 Hz and Gaussian broadening of 5 Hz were applied before Fourier transformation and line fittings were performed using the Varian built-in software. J_{PH} couplings values in PE, GPE and GPC were measured after deconvolution.

Monte-Carlo Simulations

The accuracy of AMARES and LCModel quantification was evaluated using Monte-Carlo simulations. ^{31}P brain-like unlocalized spectra were simulated at 3 Tesla using the spectral linewidth measured for each metabolite in the in vivo spectrum and concentration reported in Table 2. The distorted baseline arising from short T_2 signals (bone) was generated by summing the in vivo ^{31}P spectra from all subjects and line-broadening with a large exponential filter of 1000 Hz and Gaussian filter of 0.01 Hz.

For Monte-Carlo simulations, Gaussian noise was added to the simulated ^{31}P NMR spectra. The resulting spectra were fitted with AMARES and LCModel using the two basis sets as described above. Five different noise levels were chosen such that the peak signal-to-noise ratio (SNR) of PCr, in the frequency domain, ranged from 13 to 120. This procedure was repeated 100 times for each noise level.

Results and Discussion

^{31}P spectral pattern at 3 T

In vivo ^{31}P NMR spectra from the human occipital cortex (Figure 1) measured with the 6 cm surface coil had excellent SNR and spectral resolution and showed resonances from PCr, ATP, Pi, phosphomonoesters (PME = PE + PC), phosphodiesters (PDE = GPC + GPE). The fine multiplet structure in α-ATP and γ-ATP was not well resolved due to their shorter T_2 and to the presence of long-range ^{31}P - ^{1}H *J*-couplings (ranging between ∼2 and 8 Hz). These long-range couplings can be suppressed by using ^{1}H decoupling during acquisition (5,20) at the expense of experimental simplicity.

Spectral fitting

Initial attempts to fit ^{31}P spectra with LCModel approach #1 using the fixed linewidth basis set and default LCModel line broadening parameters resulted in large residuals for almost all resonances (Figure 1, bottom left). These residuals were caused by incorrect estimation of the spectral linewidth. By default, LCModel assumes that the line broadening applied to the basis set spectra in order to match the in vivo spectra is similar for all resonances in the

spectrum. However, in the case of ^{31}P spectra, metabolites have very different linewidths due to different T_2 relaxation times. For example, the T_2 of PCr is known to be much longer than the T_2 for the different moieties of ATP in the human brain (16,21,22) resulting in a narrower linewidth for PCr than for ATP.

Giving LCModel more flexibility to estimate the line broadening for each metabolite (LCModel approach #2), resulted in a much-improved fit with minimal residuals (Figure 1, bottom right). Previous studies using HSVD (5,6) have also shown that having flexible linewidth for each peak in the fitting algorithm helped to efficiently quantify the ^{31}P brain data. Based on the quality of the fit and residual, the basis set generated using values given in Table 1 appear suitable for analyzing ^{31}P MRS data. In addition, the fit shows that LCModel can successfully account for the distorted baseline arising from short T_2 signals (especially bone). Fitting the same spectrum with AMARES resulted in similar fit quality as with LCModel (Figure 2).

Another possible approach with LCModel (LCModel approach #3) is to incorporate information about the different linewidth for each metabolite directly into the basis set, and give less flexibility to LCModel in estimating the increase in linewidth from the basis set to the *in vivo* data. Indeed, the quality of the fit with the “adjusted linewidth” basis set and DESDT2 = 0.4 Hz (default value) was similar to that obtained with the “fixed linewidth” basis set and DESDT2 = 10 Hz (LCModel approach #2).

Monte-Carlo simulations—Although LCModel approaches #2 and #3 gave similar fit quality, the two different LCModel approaches resulted in very different quantification accuracy.

Giving LCModel too much flexibility to estimate the linewidth of each metabolite (LCModel approach #2) resulted in significant quantification bias, especially at low SNR (Figure 3) and for broad resonances such as MP and DPG. In contrast, incorporating prior knowledge of the linewidth into the basis set and setting tighter constraints (LCModel approach #3) resulted in much improved accuracy, with actual concentration values close to expected values (Figure 3).

The performance of LCModel approach #3 was similar to that of AMARES, suggesting that both algorithms are able to estimate concentrations with good accuracy, even under relatively low SNR conditions, provided that adequate prior knowledge and constraints are used. The quantification precision obtained with Monte-Carlo simulations was somewhat better with LCModel compared to AMARES (lower error bars in Figure 3). This difference in precision can be attributed to the fact that the constraints on metabolite linewidth that we used in AMARES were less tight than with LCModel. This should not be interpreted as AMARES being “less precise” than LCModel. Rather, it is a reflection that tighter constraints lead to improved precision.

In vivo metabolite concentrations

Relative metabolite concentrations obtained after LCModel and AMARES analysis are given in Figure 4 assuming a PCr concentration of 2.7 μmol/g in the healthy human brain

(6,10). PCr was used as an internal concentration reference since this peak does not overlap with other resonances (other resonances could be used, such as αATP or βATP).

Comparable relative concentrations (within SD, Figure 4A) were also observed with both methods (LCModel and AMARES) for almost all metabolites. There was an excellent correlation between the two quantification methods (r_s = 0.99, P < 0.001) as shown in Figure 4B. The absolute difference in concentrations estimated by the two methods was less than 0.2 μmol/g for all metabolites, with the exception of PDE, which was 0.26 μmol/g lower on average with AMARES than with LCModel. The highest relative difference was observed for tNAD (26.5% lower with AMARES than with LCModel, 0.56 μmol/g vs. 0.75 μmol/g), consistent with tNAD being very difficult to quantify reliably at 3 Tesla. GPE was 13% lower on average with AMARES than with LCModel. All other metabolites showed less than 12% difference between the two methods. The three above-mentioned metabolites (PDE, tNAD, GPE), were the only metabolites that showed significant differences between the two methods on our population of 10 subjects. The small differences that we observed could be due in part to small differences in baseline estimation between the two methods.

The measured Pi concentration of 1.0 μmol/g in this study is consistent with previous studies in humans (6,23). The concentration of ATP was similar to that of PCr, consistent with previously published values in human cortex (6).

Based on LCModel's output, it was also possible to measure the pH, as determined by the difference in chemical shifts between PCr and Pi (23) in this study. The measured intracellular pH in healthy brain was 7.03 ± 0.01 consistent with previously reported values (23,24). To test the reliability to measure the chemical shifts of the Pi peak at various pH, one of the in vivo spectra was manipulated such that Pi was shifted by ± 0.3 ppm (in step of 0.1 ppm) from its original chemical shift of 4.84 ppm and the resulting spectra were fitted with LCModel as described above and setting ALSDSH (i.e. standard deviation of the chemical shift) to 1.0 ppm for Pi (default value is 0.004 ppm). These shifts correspond to tissue pH values of 6.78 to 7.31, associated with pathological conditions (25,26). Results demonstrate that these shifts in Pi can be accurately picked up by LCModel (within ±0.02 ppm) thereby offering the possibility to measure changes in tissue pH. An excellent correlation was observed between the expected pH value and the pH value determined using the chemical-shift of Pi returned by LCModel (slope of 1.02, goodness-of-fit R^2 = 0.99, not shown).

In addition to fitting single voxel spectroscopy data, LCModel was also successfully employed to quantify ^{31}P MRSI data at 7 Tesla (Figure 5). Good fits were obtained even for voxels with lower SNR. The estimated concentrations from the voxel with the highest SNR (peak SNR of PCr = 56, defined as peak height divided by root mean square noise) were consistent to that measured at 3 T where Cramer-Rao Lower Bound (CRLB) < 10% for all major metabolites like PCr, Pi, ATP, PME and PDE. In the voxel with the lowest SNR (peak SNR of PCr = 16), it was possible to accurately measure PCr and ATP concentrations with CRLB < 12%. The certainty to estimate Pi was still reasonable (CRLB < 25%) while other metabolites could not be reliably determined.

Finally, to show that the described method is easily translatable to animal data, localized ^{31}P spectra acquired from mouse brain at 9.4 Tesla (19) were fitted using LCModel. The results indeed show that a good spectral fit can be obtained (Figure 6) and the measured concentrations (relative to PCr concentration of 4 μmol/g) were consistent with previously reported values (19); i.e. 2.3 μmol/g for Pi, 2.8 μmol/g for α-ATP, 1.9 μmol/g for β-ATP and 2.9 μmol/g for γ-ATP.

Conclusion

This study showed that LCModel can be used for robust fitting of in vivo ^{31}P NMR spectra (both single voxel and MRSI). This requires using adequate prior knowledge for the simulated model basis spectra as well as giving LCModel enough flexibility to account for differences in apparent metabolite linewidths (due to different T_2 relaxation times and long-range ^{31}P - ^{1}H couplings). The performance of LCModel to quantify ^{31}P MR spectra is very similar to that of AMARES. In conclusion, this study provides a new method for automated, operator-independent analysis of ^{31}P NMR spectra in the frequency domain.

Acknowledgments

This work was supported by funding from NIH grants P41EB015894, P30NS076408, R01NS38672 and R01NS070839. We would like to thank Dr. Stephen Provencher for his help on the input parameters in LCModel version 6.3 and Dr. Ivan Tkáč for providing the ^{31}P mouse spectra.

References

1. Moon RB, Richards JH. Determination of intracellular pH by 31P magnetic resonance. J Biol Chem. 1973; 248(20):7276–7278. [PubMed: 4743524]
2. Du F, Zhu XH, Qiao H, Zhang X, Chen W. Efficient in vivo 31P magnetization transfer approach for noninvasively determining multiple kinetic parameters and metabolic fluxes of ATP metabolism in the human brain. Magn Reson Med. 2007; 57(1):103–114. [PubMed: 17191226]
3. Vanhamme L, van den Boogaart A, Van Huffel S. Improved method for accurate and efficient quantification of MRS data with use of prior knowledge. J Magn Reson. 1997; 129(1):35–43. [PubMed: 9405214]
4. Hamilton G, Patel N, Forton DM, Hajnal JV, Taylor-Robinson SD. Prior knowledge for time domain quantification of in vivo brain or liver 31P MR spectra. NMR Biomed. 2003; 16(3):168–176. [PubMed: 12884361]
5. Potwarka JJ, Drost DJ, Williamson PC. Quantifying 1H decoupled in vivo 31P brain spectra. NMR Biomed. 1999; 12(1):8–14. [PubMed: 10195324]
6. Jensen JE, Drost DJ, Menon RS, Williamson PC. In vivo brain (31)P-MRS: measuring the phospholipid resonances at 4 Tesla from small voxels. NMR in Biomedicine. 2002; 15(5):338–347. [PubMed: 12203225]
7. Wang X, Lee JH. IRIS-HSVD algorithm for automatic quantitation of in vivo 31P MRS. J Magn Reson. 2009; 196(1):23–32. [PubMed: 18926748]
8. Gabr RE, Ouwerkerk R, Bottomley PA. Quantifying in vivo MR spectra with circles. J Magn Reson. 2006; 179(1):152–163. [PubMed: 16325436]
9. Slotboom J, Boesch C, Kreis R. Versatile frequency domain fitting using time domain models and prior knowledge. Magn Reson Med. 1998; 39(6):899–911. [PubMed: 9621913]
10. Kreis R, Slotboom J, Pietz J, Jung B, Boesch C. Quantitation of Localized 31P Magnetic Resonance Spectra Based on the Reciprocity Principle. J Magn Reson. 2001; 149(2):245–250. [PubMed: 11318624]

11. Provencher SW. Estimation of metabolite concentrations from localized in vivo proton NMR spectra. Magn Reson Med. 1993; 30(6):672–679. [PubMed: 8139448]
12. Frahm J, Hanefeld F. Localized proton magnetic resonance spectroscopy of cerebral metabolites. Neuropediatrics. 1996; 27(2):64–69. [PubMed: 8737820]
13. Pfeuffer J, Tkac I, Provencher SW, Gruetter R. Toward an in vivo neurochemical profile: quantification of 18 metabolites in short-echo-time ^{1}H NMR spectra of the rat brain. J Magn Reson. 1999; 141(1):104–120. [PubMed: 10527748]
14. Henry PG, Oz G, Provencher S, Gruetter R. Toward dynamic isotopomer analysis in the rat brain in vivo: automatic quantitation of 13C NMR spectra using LCModel. NMR Biomed. 2003; 16(6-7):400–412. [PubMed: 14679502]
15. Lanz B, Duarte JoMN, Kunz N, MlynÃ¡rik V, Gruetter R, Cudalbu C. Which prior knowledge? Quantification of in vivo brain 13C MR spectra following 13C glucose infusion using AMARES. Magn Reson Med. 2013; 69(6):1512–1522. [PubMed: 22886985]
16. Jung WI, Staubert A, Widmaier S, Hoess T, Bunse M, van Erckelens F, Dietze G, Lutz O. Phosphorus J-coupling constants of ATP in human brain. Magn Reson Med. 1997; 37(5):802–804. [PubMed: 9126956]
17. Govindaraju V, Young K, Maudsley AA. Proton NMR chemical shifts and coupling constants for brain metabolites. NMR Biomed. 2000; 13(3):129–153. [PubMed: 10861994]
18. Naressi A, Couturier C, Devos JM, Janssen M, Mangeat C, Beer Rd, Graveron-Demilly D. Java-based graphical user interface for the MRUI quantitation package. Magma. 2001; 12(2-3):141–152. LA - English. 10.1007/BF02668096 [PubMed: 11390270]
19. Tkac I, Henry PG, Zacharoff L, Wedel M, Gong W, Deelchand DK, Li T, Dubinsky JM. Homeostatic adaptations in brain energy metabolism in mouse models of Huntington disease. JCBFM. 2012; 32(11):1977–1988.
20. Luyten PR, Bruntink G, Sloff FM, Vermeulen JW, van der Heijden JI, den Hollander JA, Heerschap A. Broadband proton decoupling in human 31P NMR spectroscopy. NMR Biomed. 1989; 1(4):177–183. [PubMed: 2641284]
21. Merboldt KD, Chien D, Hanicke W, Gyngell ML, Bruhn H, Frahm J. Localized 31P NMR spectroscopy of the adult human brain in vivo using stimulated-echo (STEAM) sequences. J Magn Reson. 1969; 89(2):343–361.
22. Lei H, Zhu XH, Zhang XL, Ugurbil K, Chen W. In vivo 31P magnetic resonance spectroscopy of human brain at 7 T: An initial experience. Magn Reson Med. 2003; 49(2):199–205. [PubMed: 12541238]
23. Mason GF, Chu WJ, Vaughan JT, Ponder SL, Twieg DB, Adams D, Hetherington HP. Evaluation of 31P metabolite differences in human cerebral gray and white matter. Magn Reson Med. 1998; 39(3):346–353. [PubMed: 9498589]
24. Barker PB, Butterworth EJ, Boska MD, Nelson J, Welch KMA. Magnesium and pH imaging of the human brain at 3.0 Tesla. Magn Reson Med. 1999; 41(2):400–406. [PubMed: 10080290]
25. Adler S, Simplaceanu V, Ho C. Brain pH in acute isocapnic metabolic acidosis and hypoxia: a 31P-nuclear magnetic resonance study. Am J Physiol. 1990; 258(1):F34–F40. [PubMed: 2301594]
26. Rottenberg DA, Ginos JZ, Kearfott KG, Junck L, Dhawan V, Jarden JO. In vivo measurement of brain tumor pH using [11C]DMO and positron emission tomography. Ann Neurol. 1985; 17(1): 70–79. [PubMed: 3872621]
27. Lu M, Zhu XH, Zhang Y, Chen W. Intracellular redox state revealed by in vivo 31P MRS measurement of NAD+ and NADH contents in brains. Magn Reson Med. 201310.1002/mrm.24859.

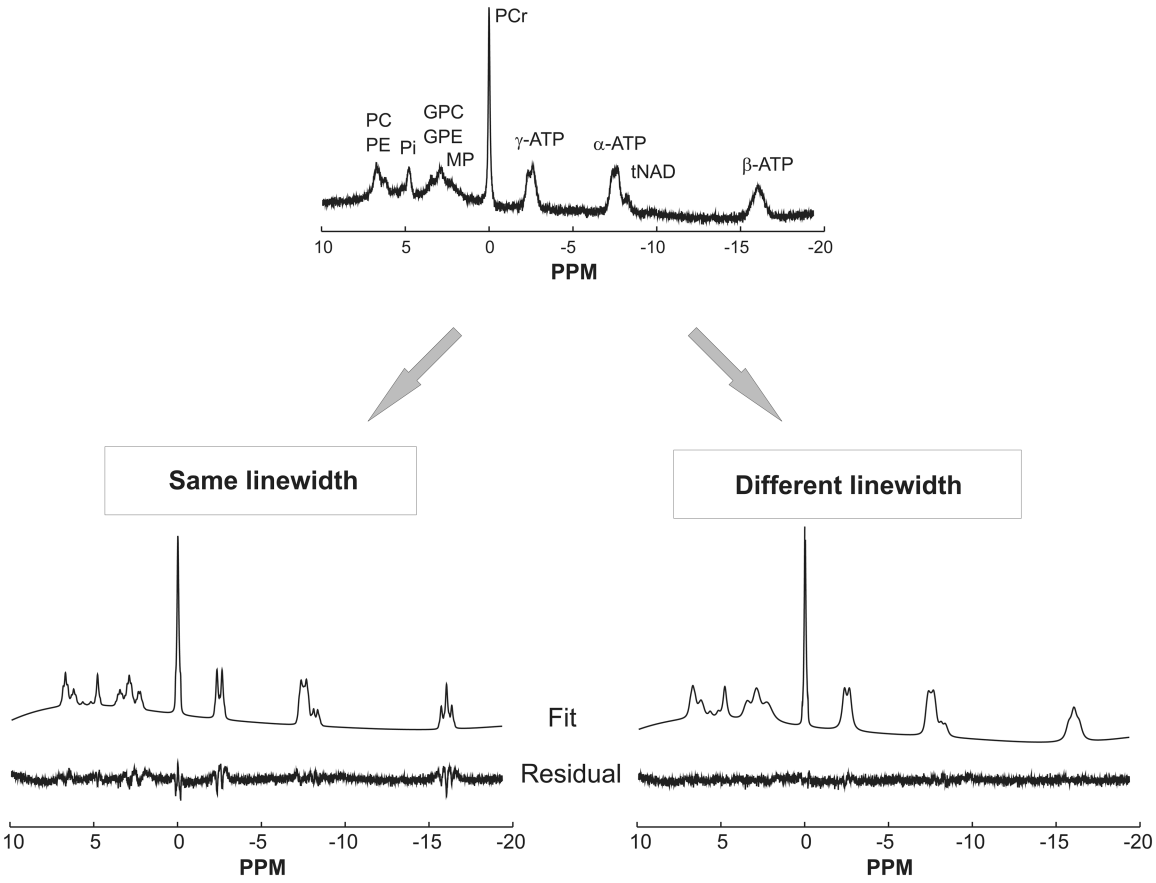

Figure 1.

LCModel fits of a ^{31}P spectrum (T_R = 2 s, 600 averages, peak SNR of PCr = 81, no apodization) obtained by constraining the linewidth to be similar for all metabolites using LCModel approach #1 (left) or allowing the linewidth to vary using LCModel approach #2 (right). The root mean square of fit residuals was almost 65% higher in the first case.

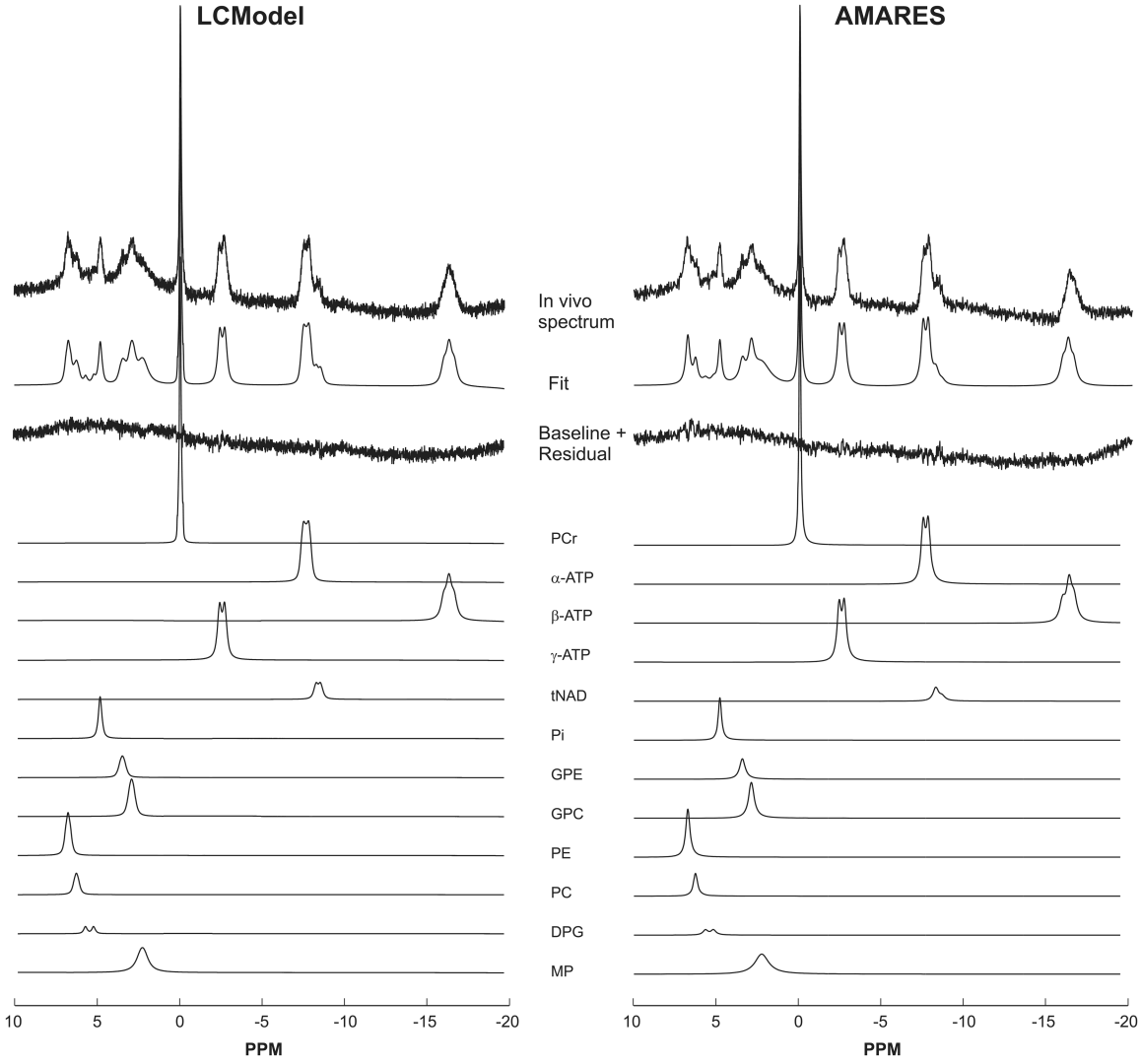

Figure 2.

Comparison of ^{31}P spectra fitted using LCModel (left) and AMARES (right). No baseline correction was applied before fitting. The fits were very similar.

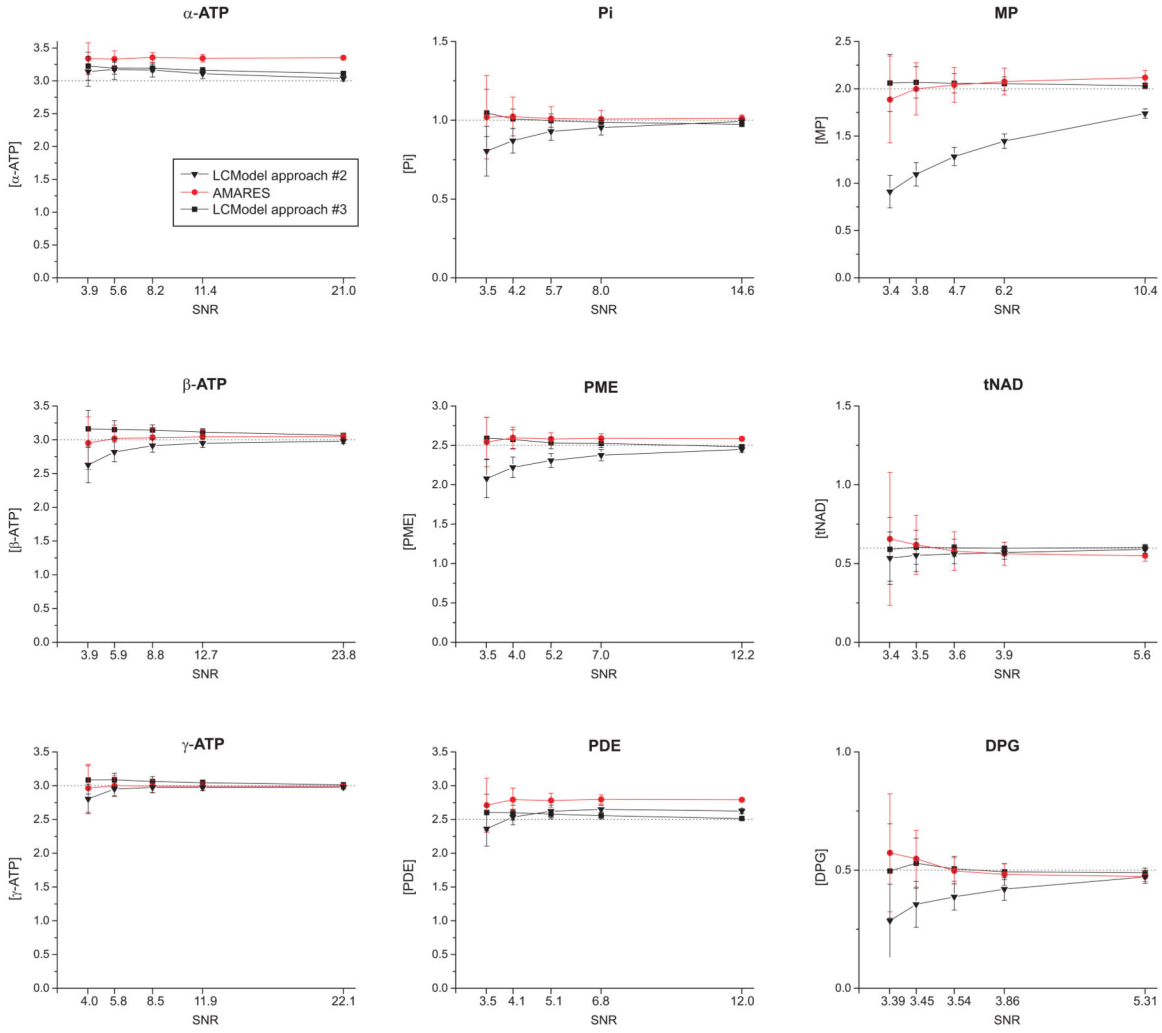

Figure 3.

Accuracy of quantification of ^{31}P metabolite concentrations (in μmol/g) at various SNR levels determined using Monte-Carlo simulations. For each metabolite, five data points are shown, corresponding to the five SNR conditions used in Monte-Carlo-simulations. The corresponding peak SNR of PCr for the five data points were: 13 (a), 24 (b), 40 (c), 61 (d) and 120 (e). All concentrations are relative to [PCr] of 3 μmol/g. Dotted lines represent the expected concentrations (values used to simulate ^{31}P spectra). LCModel approach #2 uses the “fixed linewidth” basis set with DEEXT2 = 10 Hz and DESDT2 = 10 Hz, and LCModel approach #3 uses the “adjusted linewidth” basis set with default values of DEEXT2 = 2 Hz and DESDT2 = 0.4 Hz.

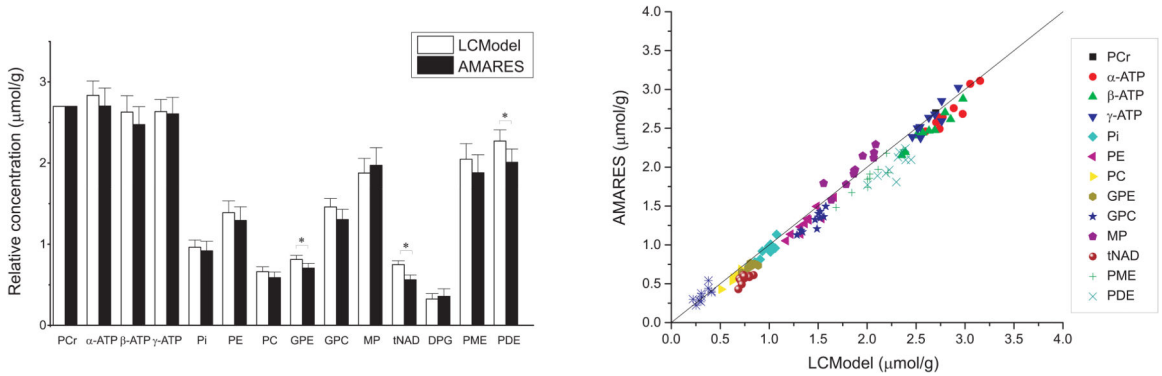

Figure 4.

Comparison of mean relative ^{31}P concentrations (in μmol/g) obtained with LCModel and AMARES (left) using PCr as a concentration reference of 2.7 μmol/g. * represents $P < 0.05$ after Bonferroni correction and error bars represent SD. Excellent correlation was observed between the two methods for almost all metabolite concentrations (right).

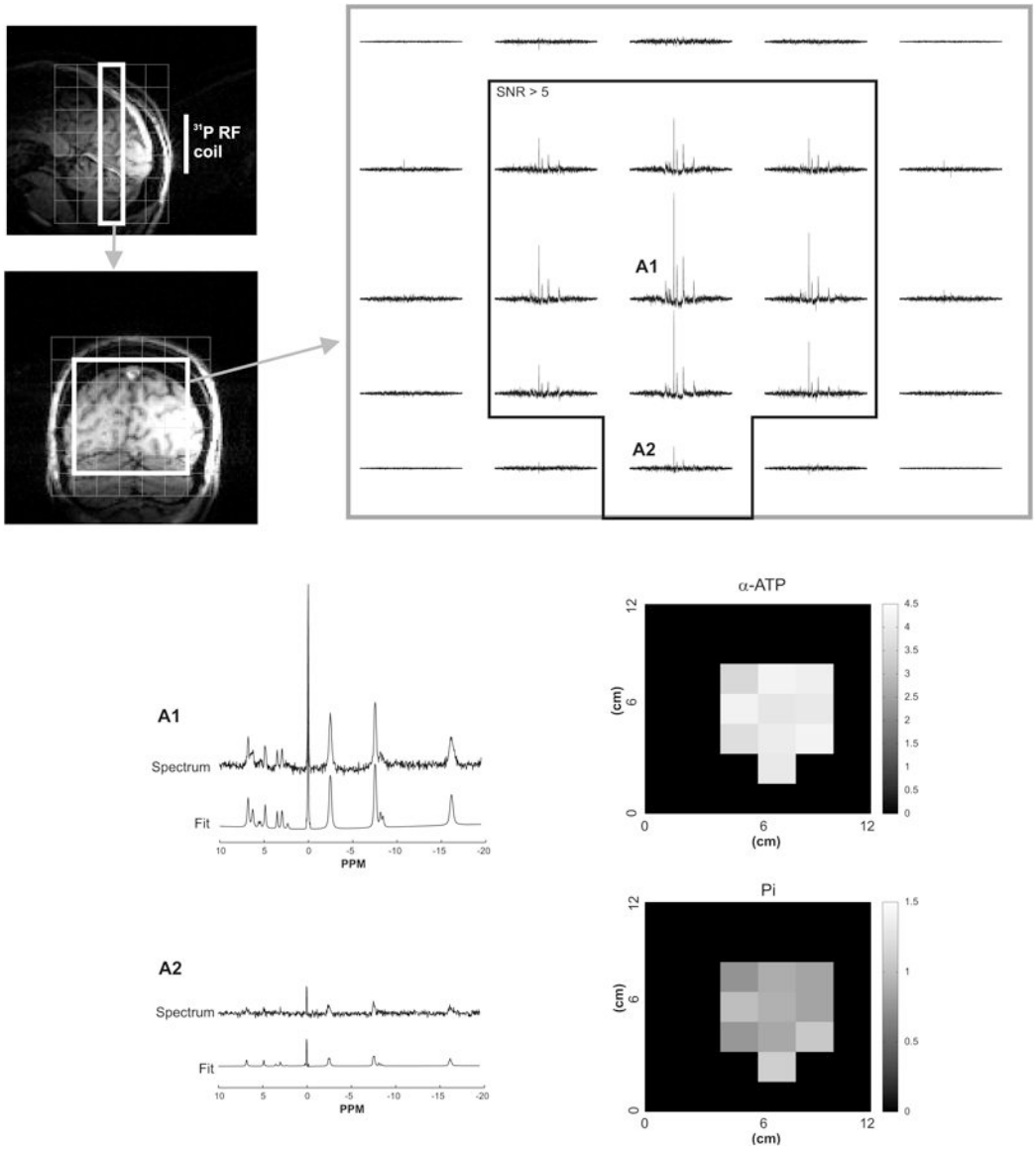

Figure 5.

Example of LCModel analysis of ^{31}P MRSI data acquired in one human subject at 7 T. The 5×5 spectral grid shows spectra from the central part of a coronal slice (white box on T_1-weighted sagittal and coronal images). LCModel fits are shown for two different voxel locations (denoted as A1 and A2). Voxels where the SNR of PCr was greater than 5 (shown by the black box on the 5×5 spectral grid) were used to generate the concentration maps (in μmol/g) for α-ATP and Pi as determined by LCModel.

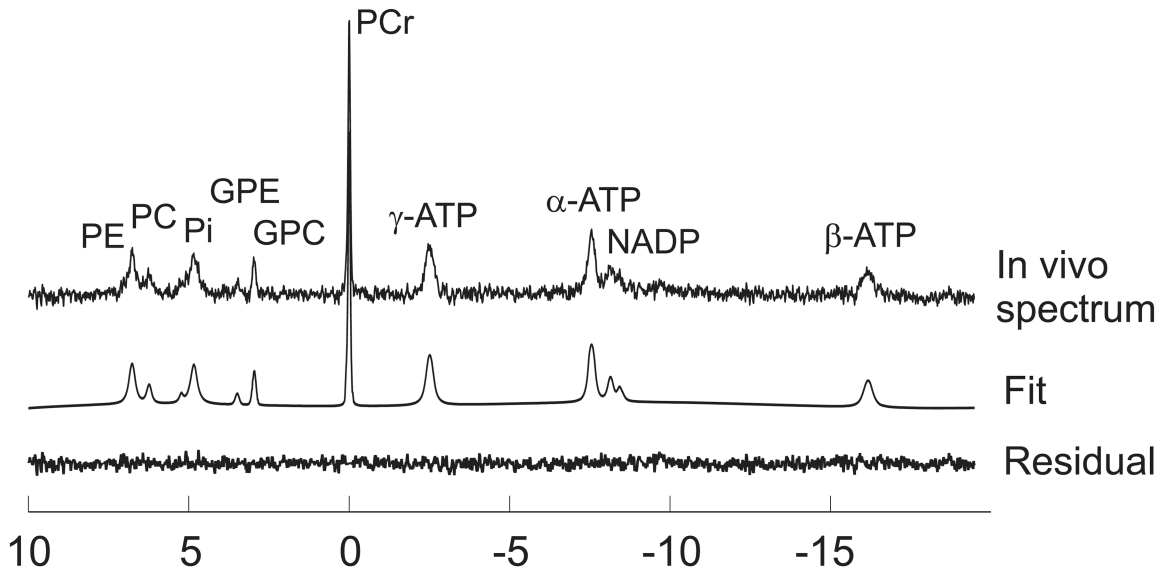

Figure 6.

LCModel fit of localized in vivo ^{31}P spectra from mice brain at 9.4 T; summed data from 4 animals, ISIS localization technique, VOI = 75 μl, T_R = 5.3 sec; 2496 averages, line broadening of 2 Hz and Gaussian filtering of 1.25 Hz.

Table 1

Chemical shift and *J*-coupling constants used to simulate the ^{31}P basis model spectra.

Metabolites	Chemical shift (ppm)	J_{PP} coupling (Hz)	J_{PH} coupling (Hz)	References
PCr	0			
α-ATP	-7.56‡	$J_{P_\alpha-P_\beta}$ = 16.30	$J_{P_\alpha-H_4}$ = 1.90	(16,17,27)
β-ATP	-16.18	$J_{P_\alpha-P_\gamma}$ = 15.40	$J_{P_\alpha-H_5}$ = 6.50	
γ-ATP	-2.53		$J_{P_\alpha-H'_5}$ = 4.90	
Pi	4.84			(16)
PC	6.23†		J_p-H_1 = 6.30	(17)
			$J_p-H'_1$ = 6.25	
PE	6.77		$J_p-H_1 = J_p-H'_1$ = 6.89	†
GPC	2.94		$J_p-H_3 = J_p-H'_3$ = 6.08	†
			$J_p-H_7 = J_p-H'_7$ = 6.08	
GPE	3.49		$J_p-H_3 = J_p-H'_3$ = 6.23	†
			$J_p-H_7 = J_p-H'_7$ = 6.23	
DPG	5.71			(5)
	5.23			
MP	2.30			
NADH	-8.13			(27)
NAD^+	-8.31	$J_{P-P'}$ = 16.30		

‡measured from ^{31}P MRS acquired in human brain at 7 T.

†measured from brain extract.

Table 2

Spectral linewidth and concentration of metabolites used in Monte-Carlo simulation.

Metabolites	Concentration (μmol/g)	Linewidth (Hz)
PCr	3	3
α-ATP	3	9
β-ATP	3	18
α-ATP	3	13
Pi	1	10
PC	1.5	11
PE	1	10
GPC	1.5	12
GPE	1	11
DPG	0.5	10
MP	2	33
NADH	0.5	4
NAD^+	0.1	12